Systematics in the ionization states of ^{57}Fe following the electron-capture decay of ^{57}Co in different rare-gas matrices

M. Van der heyden, H. Micklitz,* S. Bukshpan,† and G. Langouche
Instituut voor Kern-en Stralingsfysika, University of Leuven, B-3030 Leuven, Belgium
(Received 14 October 1986)

The ^{57}Fe Mössbauer emission spectra of ^{57}Co implanted in the rare-gas matrices Ne, Ar, Kr, Xe, and the rare-gas mixture Ar + 10 at. % Xe show systematic behavior in the ionization states of ^{57}Fe following the electron-capture decay of ^{57}Co. This systematic behavior can be explained by a charge transfer process via resonant tunneling between the Fe ion and one of its rare-gas nearest neighbors. The recombination with "free" electrons is found to be important in the Xe matrix only. A new $\Delta\langle r^2\rangle$ value is given for the Mössbauer transition in ^{57}Fe.

I. INTRODUCTION

Mössbauer-effect (ME) experiments with rare-gas-matrix–isolated (RGMI) atoms have been performed since 1971 in order to study the hyperfine (hf) interaction of "almost-free" atoms.[1] These ME *absorber* experiments were followed later by some ME experiments where the doped RG matrix has been used as a ME *source*, i.e., where radioactive atoms have been incorporated into the RG matrix.[1–3] Generally speaking, such ME source experiments with insulating solids provide the possibility to study so-called decay aftereffects. The experiments with ^{57}Co in a xenon matrix, for example, gave evidence for the formation of $Fe^+(3d^7)$ ions after the electron-capture (EC) decay of ^{57}Co in Xe.[2,3] Such charged states, when treated as "almost-free" ionic states, provide further isomer-shift calibration points in case self-consistent Dirac-Fock-Slater calculations for these ionic configurations are available. In order to understand the mechanisms leading to the stabilization of charged states in RG matrices in more detail, and eventually to obtain further isomer-shift calibration points for ^{57}Fe, we have performed systematic studies of the EC decay of ^{57}Co in the RG matrices Ne, Ar, Kr, and the RG mixture Ar+10 at. % Xe.

II. EXPERIMENTAL DETAILS

The ^{57}Co(RG) Mössbauer-effect sources were obtained by the codeposition of ^{57}Co ions, emerging from an ion accelerator followed by a mass separator with an energy of $\simeq$85 keV, and the RG matrix gas onto a cold (usually 4.2 K) substrate. The experimental setup is shown in Fig. 1. The numbers in the following description refer to the numbers given in Fig. 1.

The sample preparation is made in an ultrahigh vacuum (UHV) system. The residual gas pressure is 10^{-6} Pa without and 10^{-7} Pa with liquid He in the cryostat (7). The substrate of the ^{57}Co(RG) ME source is a variable-temperature cold finger (1), covered with an aluminum foil and surrounded by a liquid-nitrogen-cooled radiation shield (4). The substrate makes an angle of 45° with the absorber (2) and with the ion beam emerging from the liquid-nitrogen-cooled beam line (5), connecting the ion separator to the cryostat. The vacuum in the beam-line system is 10^{-5} Pa. It can be separated from the cryostat after ion implantation by an UHV valve (9). The RG matrix gas (purity: 99.99% for Ne, 99.9997% for Ar, and 99.997% for Kr) enters the cryostat through an adjustable needle valve and emerges from a stainless-steel capillary (6) ($\simeq$1 mm inner diameter) parallel to the ^{57}Co beam. Typical RG deposition rates were 5–10 nm/s, resulting in a RG pressure during deposition of $\simeq 10^{-4}$ Pa. Before starting the ^{57}Co deposition, the beam direction is adjusted by an electrostatic deflection system (8) to optimize the sputtering rate (measured by the increase of the RG pressure) by ^{59}Co ions ($\simeq 10^{13}$ ions cm^{-2} s^{-1}). The ^{57}Co-ion-beam intensity varied between 5×10^9 and 2×10^{10} ions cm^{-2} s^{-1}. The resulting ^{57}Co(RG) ME sources had a typical thickness of 50 μm and an ^{57}Co atomic concentra-

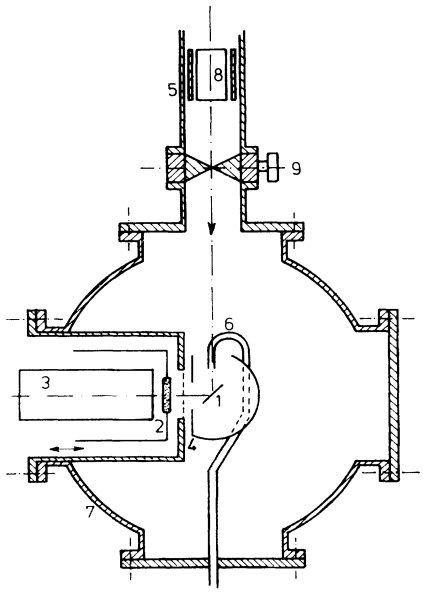

FIG. 1. Experimental setup used for the ^{57}Co implantation experiments. The numbers given are referred to in the text.

tion of 10^{-8}. The distance between implanted source and absorber [sodium ferrocyanide (SFC), 1 mg/cm^2 ^{57}Fe], moving outside the cryostat, is ≈ 3.5 cm. The γ detector used is a Kr proportional counter (3). The counting rate ranged from 150 Hz for Kr and Ne to 1 kHz for Ar. The ^{57}Fe ME spectra were recorded in 3–7 d.

III. RESULTS

^{57}Co was implanted in the RG matrices Ne, Ar, and Kr and a RG mixture of Ar with about 10 at. % Xe.[4] The ^{57}Fe ME emission spectra are shown in Figs. 2–4. All hf data obtained from least-squares fits to the measured spectra in Figs. 2–4, together with the ^{57}Co(Xe) data from Refs. 2 and 3, are summarized in Table I.

The ^{57}Co(Ne) emission spectrum shown in Fig. 2 can be fitted with a single line and a quadrupole doublet, both having the *same* isomer shift. The spectrum, therefore, can be interpreted as that due to only ionization state of Fe, but with two different lattice sites, one a cubic, the other a distorted, or defect-associated, noncubic site. However, we cannot exclude another possibility, namely, that the spectrum is instead a paramagnetic relaxation spectrum of one ^{57}Fe state on *one* lattice site only. The isomer-shift value of this ^{57}Fe state lies between those of $(^{57}Fe^{+})^{*}(3d^{7})$ (Refs. 2 and 3) and $^{57}Fe^{+}(3d^{6}4s)$ (Refs. 5 and 6). It is interpreted as that of a highly excited $(^{57}Fe^{2+})^{*}(3d^{6})$ or an $^{57}Fe^{3+}(3d^{5})$ state as will be discussed in detail in Sec. IV B.

The ^{57}Co(Ar) spectrum at a matrix temperature of 4.2 K (see Fig. 3) shows a paramagnetically split $(Fe^{+})^{*}(3d^{7})$ state due to Fe^{+} ions on a cubic lattice site with an isotropic hyperfine interaction,[7] and, in addition, an $Fe^{+}(3d^{6}4s)$ state on a noncubic lattice site, as indicated by the isomer-shift value[5,6] and the quadrupole splitting (QS). The observed value of the QS (see Table I) is in excellent agreement with the theoretical value for the $Fe^{+}(3d^{6}4s)$ crystal-field ground state (Kramers doublet) as calculated in Ref. 6. At a matrix temperature of 17 K the paramagnetically split $(Fe^{+})^{*}(3d^{7})$ spectrum collapses to a single line (see Fig. 4) due to fast spin-lattice relaxation.

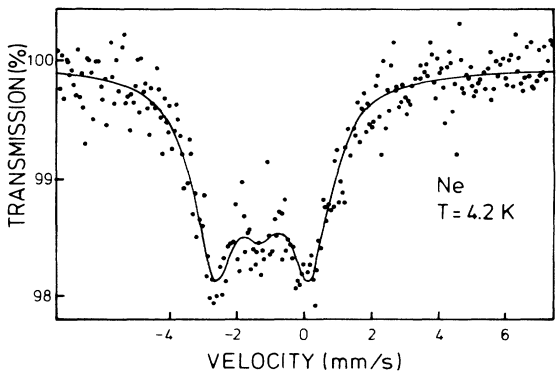

FIG. 2. ^{57}Fe ME emission spectrum of ^{57}Co in a Ne matrix at 4.2 K. Doppler velocity is given relative to a SFC absorber at 300 K.

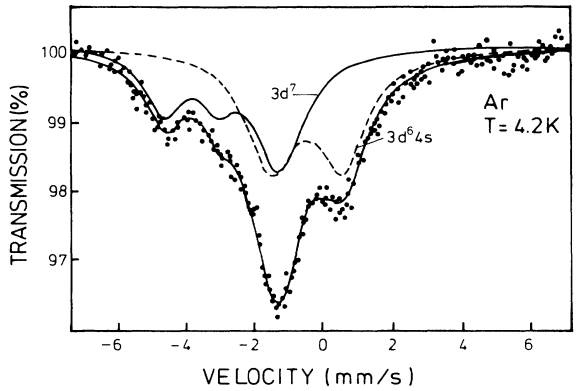

FIG. 3. ^{57}Fe ME emission spectrum of ^{57}Co in an Ar matrix at 4.2 K. Doppler velocity is given relative to a SFC absorber at 300 K.

Isomer-shift values and quadrupole splitting do not change between $T = 4.2$ and 17 K.

The ^{57}Co(Kr) spectrum can be fitted with a paramagnetically split $(^{57}Fe^{+})^{*}(3d^{7})$ component with an effective hyperfine coupling constant $(a_g)_{\text{eff}}$, reduced with respect to a_g for the nuclear ground state of $(^{57}Fe^{+})^{*}(3d^{7})$ in Ar

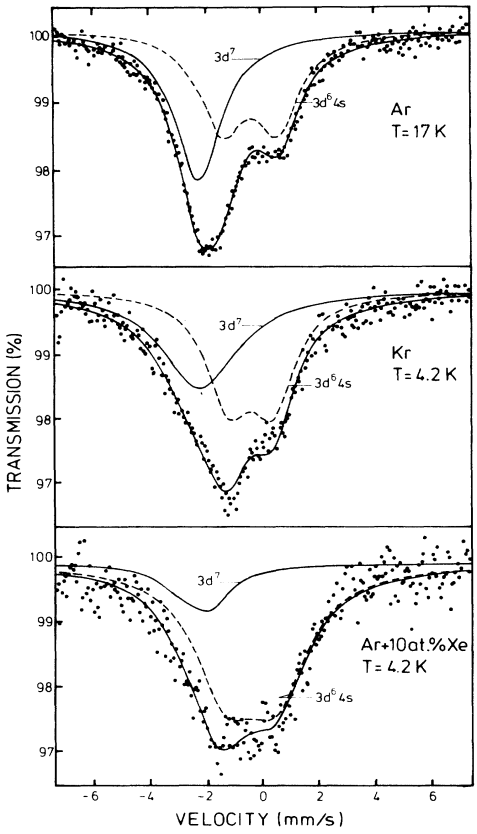

FIG. 4. ^{57}Fe ME emission spectra of ^{57}Co in an Ar matrix at 17 K, a Kr matrix at 4.2 K, and an Ar+10 at. % Xe mixture at 4.2 K. Doppler velocity is given relative to a SFC absorber at 300 K.

TABLE I. Summary of all hf data from ^{57}Co(RG) experiments as obtained from least-squares fits to the ^{57}Fe ME emission spectra shown in Figs. 2–4. The hf data for ^{57}Co(Xe) are from Ref. 2. Isomer shift (IS), quadrupole splitting (QS), effective hf coupling constant $[(a_g)_{\text{eff}}]$, and linewidth (Γ) are all given in mm/s. The relative intensities I of the corresponding ^{57}Fe states are given in %.

	Ne, 4.2 K		Ar		Kr	Ar+10 at. % Xe	Xe		Assigned
	Site 1	Site 2	4.2 K	17 K	4.2 K	4.2 K	4.2 K	20.5 K	configuration
IS	1.15(2)	1.18(4)							$(^{57}Fe^{2+})^*(3d^6)$
QS	2.8(2)								or
Γ	1.6(1)	1.6(1)							$^{57}Fe^{3+}(3d^5)$
I	80(8)	20(8)							
IS			2.1(1)	2.1(1)	1.9(2)	2.1(1)	1.77(8)	1.77(8)	$(^{57}Fe^{+})^*(3d^7)$
$(a_g)_{\text{eff}}$			1.6(1)		0.8(1)	0.5(1)			
Γ			1.4(1)	2.0(2)	2.8(3)	1.8(2)	1.4	0.7	
I			47(5)	47(5)	46(5)	15(5)	70	60	
IS			0.32(10)	0.32(10)	0.3(1)	0.3(1)			$^{57}Fe^{+}(3d^6 4s)$
QS			2.1(1)	2.0(1)	1.7(2)	1.8(2)			
Γ			1.8(1)	1.9(1)	2.1(2)	2.7(3)			
I			53(5)	53(5)	54(5)	85(5)			
IS							−0.76(2)	−0.76(2)	$^{57}Fe(3d^6 4s^2)$
Γ							0.6	0.6	
I							30	40	

due to paramagnetic relaxation, and again an $^{57}Fe^{+}(3d^6 4s)$ state on a noncubic lattice site. Since we did *not* fit the $(^{57}Fe^{+})^*(3d^7)$ component with a *relaxation* spectrum, the least-squares fit to this spectrum is not too good.

The ^{57}Co(Ar+10 at. % Xe) spectrum shows the same components as those of ^{57}Co(Ar) and ^{57}Co(Kr), however, with a different $Fe^{+}(3d^6 4s)$-to-$(Fe^{+})^*(3d^7)$ intensity ratio. This ratio is about 1 in Ar and Kr but a factor of about 3 larger in the Ar+10 at. % Xe mixture. The effective paramagnetic splitting of the $(^{57}Fe^{+})^*(3d^7)$ state again decreases on going from Kr to Ar+10 at. % Xe, indicating a decrease in the spin-lattice relaxation time going from Ar to Kr and further to Xe.[8]

Except for Xe,[2,3] the $^{57}Fe(3d^6 4s^2)$ state is not seen after the EC decay of ^{57}Co in any of the RG matrices investigated.

IV. DISCUSSION

A. Ionization states of Fe

As ^{57}Co decays via EC to Fe, 73% of the resulting Fe will be present as Fe^{n+}, with $n \geq 3$.[9] If the Fe^{n+} ions are embedded in a RG matrix, their ionization state can be reduced by electron donation of a neighboring RG atom as long as this process is energetically favorable, e.g.,

$$Fe^{n+} + RG \xrightarrow{\tau_t} Fe^{(n-1)+} + RG^{+} + \Delta E$$

with $\Delta E \geq 0$. The time scale τ_t of the charge transfer process is generally assumed to be much shorter than the lifetime τ_γ of the nuclear excited state of ^{57}Fe, i.e. $\tau_t \ll \tau_\gamma = 10^{-7}$ s. The energy mismatch ΔE is equal to the difference between the energy released as a consequence of the reduction of the ionization state of Fe and the ionization energy of the RG atom (see Fig. 5). For $n \geq 3$, in all RG matrices, the energy mismatch ΔE is positive (the ionization energies of Fe^{n+} are taken from Ref. 10), i.e., the Fe^{n+} ions will be reduced to Fe^{2+}.

For a further reduction to Fe^{+}, ΔE is no longer positive in Ne, but still is in Ar, Kr, and Xe (see Fig. 5). This conclusion fits with the experimentally observed ionization state of Fe in Ne which is probably an excited state of Fe^{2+} or maybe Fe^{3+} (see below). In Ar, Kr, and Xe a reduction to Fe^{+} is energetically possible. Indeed only

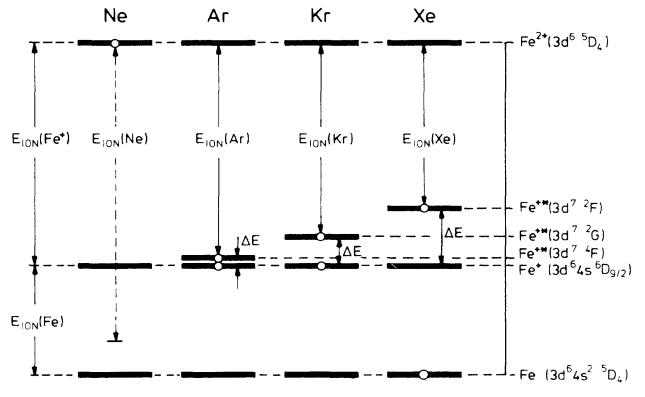

FIG. 5. Comparison of the Fe and Fe^{+} ionization energies with those of the different RG atoms. The energy scale at the right-hand side shows in addition the excited Fe^{+} states which are occupied in a charge transfer process via resonant tunneling as described in the text. The circles represent the ^{57}Fe states found in the ^{57}Fe ME emission spectra shown in Figs. 2–4 and in Refs. 2 and 3.

Fe^+ states are found in Ar, Kr, and Ar+10 at. % Xe. In order to answer the question why we observe two different Fe^+ states in these RG matrices (see Fig. 4), we have to look in more detail how the electron transfer between Fe^{2+} and one of its RG ligands occurs.

We assume that this charge transfer process takes place via a resonant tunneling process to an excited state of Fe^+. The mismatch energy ΔE (see Fig. 5) remains with the Fe^+ state, until this excited $(Fe^+)^*$ state decays via photon emission to the $Fe^+(3d^6 4s\ ^6D_{9/2})$ ground state. A phonon-assisted electron transfer to the Fe^+ ground state is very unlikely since the mismatch energy $\Delta E \gg \hbar\omega_D$ (ω_D is the Debye frequency of the RG matrix). The excited $(Fe^+)^*$ state, occuring after the charge transfer process in the different RG matrices, thus is an $(Fe^+)^*(3d^7\ ^4F)$ state in Ar, an $(Fe^+)^*(3d^7\ ^2G)$ state in Kr, and an $(Fe^+)^*(3d^7\ ^2F)$ state in Xe.[10] All these states and all other lower excited states of Fe^+ have the *same* parity as the Fe^+ ground state,[10] therefore forbidding electric dipole transitions between these states and stabilizing the $(Fe^+)^*(3d^7)$ states for times much longer than τ_γ. Only if the Fe^+ lattice site has no inversion symmetry, are these transitions allowed and they may occur within the nuclear lifetime.

The ^{57}Fe ME spectra in Fig. 2 show both Fe^+ states ($3d^7$ and $3d^6 4s$) in the RG matrices Ar, Kr, and Ar+10 at. % Xe, while only $(Fe^+)^*(3d^7)$ is found in Xe.[2,3] The $Fe^+(3d^6 4s)$ component always exhibits a relatively large quadrupole splitting, while such a splitting is not observable for the $(Fe^+)^*(3d^7)$ state.[11] The lattice sites of the $Fe^+(3d^6 4s)$ ions, therefore, are distorted or defect associated and it is likely that, as a consequence of this, the site symmetry has no inversion center. At these lattice sites the $(Fe^+)^*(3d^7)$ states obtained after charge exchange with one of its RG ligands will immediately decay via photon emission to the $Fe^+(3d^6 4s)$ ground state.

This model is supported by the fact that the $Fe^+(3d^6 4s)$-to-$(Fe^+)^*(3d^7)$ intensity ratio is much larger in the Ar+10 at. % Xe mixture than in the pure Ar matrix (3.3 and 1.2 respectively): the presence of substitutional Xe in the Ar matrix breaks the inversion symmetry in the nearest-neighbor shell of the $(Fe^+)^*(3d^7)$ ions, thus enhancing the $(Fe^+)^*(3d^7) \rightarrow Fe^+(3d^6 4s)$ transition.

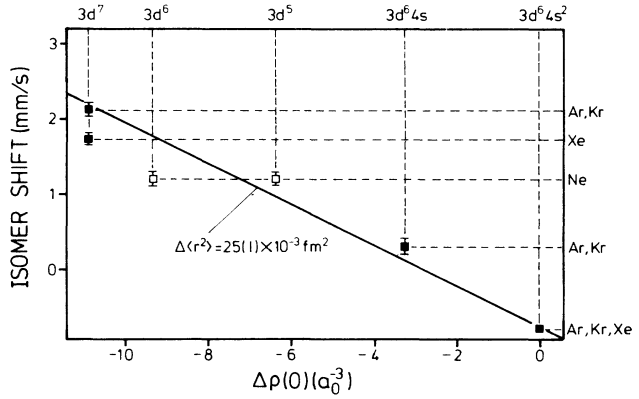

FIG. 6. Isomer shift vs electron density $\rho(0)$ plot for different states of ^{57}Fe observed in RGMI experiments. The isomer shift of $(^{57}Fe^+)^*(3d^7)$ in Xe is from Ref. 2, the isomer shift of $^{57}Fe(3d^6 4s^2)$ from Ref. 8. All isomer shifts are absorber isomer shifts given relative to α-Fe at 300 K. $\Delta\rho(0)$ values taken from Ref. 19 are given relative to $Fe(3d^6 4s^2)$.

The appearance of two different Fe^+ lattice sites in Ar and Kr but not in Xe is analogous to the findings of other authors from ESR studies of RGMI atoms: Li,[12,13] Na,[12,13] and Al atoms,[14,15] for example, occupy several lattice sites in Ne, Ar, and Kr but only one site in Xe.

The reduction of Fe^+ to Fe, occuring in Xe only, proceeds by means of electron conduction. This statement is supported by three facts: (i) the reduction rate of Fe^+ in Xe is proportional to $\sqrt{T}$, e.g., to the thermal velocity of free electrons,[2] (ii) solid Xe is the best conductor of all RG matrices,[16] and (iii) the Ar+10 at. % Xe mixture does *not show* $^{57}Fe(3d^6 4s^2)$. Since an atomic concentration of 10% is below the percolation threshold, the reduction of Fe^+ to Fe will not occur if it is due to a collective process, e.g., due to the band structure of Xe.

B. ^{57}Fe isomer-shift calibration

In former matrix-isolation work the points used for calibrating the isomer shift of ^{57}Fe against the electron density $\rho(0)$ at the Fe nucleus, were the isomer shift of $^{57}Fe^+(3d^7)$ in Xe,[2] $^{57}Fe^+(3d^6 4s)$ in a Xe-HI mixture,[5,6] and $^{57}Fe(3d^6 4s^2)$ in Xe,[8] together with a non-matrix-isolation result for $^{57}Fe^{2+}(3d^6)$, namely FeF_2.[17] The Dirac-Fock-Slater (DFS) electron-density calculations for these free ions were performed by Shenoy.[18]

Comparing our newly obtained isomer-shift values to those mentioned above, we come to the following conclusions: (i) the $^{57}Fe^+(3d^6 4s)$ isomer shift in Ar and Kr is within the experimental errors the same as that found for ^{57}Fe in a Xe-HI matrix after uv irradiation;[5,6] (ii) the isomer shift of $(^{57}Fe^+)^*(3d^7)$ reduces from +2.1(1) mm/s in Ar to +1.77(8) mm/s in Xe (isomer shift values relative to α-Fe at 300 K),[2,3] indicating a lower electron density at the Fe nucleus in Ar than in Xe. We will take the isomer shift of $(^{57}Fe^+)^*(3d^7)$ in Ar as a new isomer-shift calibration point and suggest that the lower isomer-shift value in Xe is due to the following effect: the $(^{57}Fe^+)^*(3d^7\ ^2F)$ state occupied in Xe (see Fig. 5) is a relative high excited state ($\Delta E \simeq 4$ eV for Xe compared to only $\simeq 0.4$ eV for Ar). The $3d$-shielding effect, therefore, will be reduced, leading to an increase in the electron density $\rho(0)$ at the Fe nucleus; matrix effects are excluded to be responsible for the isomer-shift difference between $(Fe^+)^*(3d^7)$ in Ar and Xe, respectively, since we do not see such a difference for the $^{57}Fe^+(3d^6 4s)$ ground state.

The interpretation of the isomer shift observed in Ne is somewhat problematic. If this isomer shift is interpreted as that of $^{57}Fe^{2+}(3d^6)$ and if its isomer shift, together with those of the other matrix-isolation calibration points, is plotted against DFS electron densities calculated by Reschke, Trautwein, and Desclaux,[19] this isomer-shift calibration point falls totally out of the trend followed by the other calibration points (see Fig. 6). Therefore we suggest again that the reason for this is the fact that Fe^{2+} in Ne is in a highly excited metastable $3d^6$ state (the

mismatch energy ΔE in the charge transfer process $Fe^{3+}+Ne \rightarrow Fe^{2+}+Ne$ is $\Delta E \simeq 9$ eV; all excited $3d^6$ states up to $\simeq 6$ eV are metastable states[10], strongly reducing the $3d$-shielding effect.

A completely different interpretation of the ^{57}Fe isomer shift observed in Ne is the following: if we take this isomer-shift value as that of $^{57}Fe^{3+}(3d^5)$ this value would be rather close to the isomer-shift calibration line interpolated from the other isomer-shift calibration points (see Fig. 6). Therefore the question arises whether the charge transfer model described in Sec. IV A, allows the observation of an Fe^{3+} state despite the fact that an Fe^{2+} state would be energetically more favorable. This, indeed, is possible if the charge transfer time τ_t is much longer than the nuclear lifetime τ_γ. Such a large τ_t can be expected only if there are no excited Fe^{2+} states available to allow a *resonant* charge transfer process. Unfortunately, energy levels for Fe^{2+} with an excitation energy higher than 6 eV are not documented.[10] For this reason the interpretation of the ^{57}Fe isomer shift in Ne remains open: it is either due to a highly excited $(^{57}Fe^{2+})^*(3d^6)$ or the $^{57}Fe^{3+}(3d^5)$ state.

Summarizing, we have three isomer-shift calibration points: $(^{57}Fe^{+})^*(3d^7)$ in Ar, a new calibration point; $^{57}Fe^{+}(3d^6 4s)$ in Ar, Kr, (this work) and in Xe;[5,6] $^{57}Fe(3d^6 4s^2)$ as given in Ref. 8. Taking these isomer-shift values and the $\rho(0)$ values as calculated by Reschke, Trautwein, and Desclaux[19] we obtain $\Delta\langle r^2\rangle = 25(1)\times 10^{-3}$ fm^2. The calibration curve is shown in Fig. 6. For convenience also the isomer shift observed in Ne and the $\rho(0)$ values for $Fe^{2+}(3d^6)$ and $Fe^{3+}(3d^5)$ are given.

Our new $\Delta\langle r^2\rangle$ value is only slightly larger than that given in Ref. 2 [$\Delta\langle r^2\rangle = 22.2(8)\times 10^{-3}$ fm^2] but much larger than that in Ref. 5 [$\Delta\langle r^2\rangle = 14.1(7)\times 10^{-3}$ fm^2]. All those values were obtained with the help of isomer-shift calibration points from RGMI experiments. The reason for the large discrepancy between our new $\Delta\langle r^2\rangle$ value and that in Ref. 5 essentially lies in the fact that the $\rho(0)$ values for the individual Fe configurations used in this paper and in Ref. 2 are quite different from those used in Ref. 5. The new $\Delta\langle r^2\rangle$ value, is in rather good agreement with that found from lifetime measurements of the ^{52}Fe EC decay [$\Delta\langle r^2\rangle = 33(3)\times 10^{-3}$ fm^2 (Ref. 20)].

V. CONCLUSION

Systematic studies of the EC decay of ^{57}Co in the different RG matrices (Ne, Ar, Kr, Ar+10 at.% Xe) enabled us to develop a consistent model to explain the occurence of different ionization states in these RG matrices. This model essentially is based on a charge transfer process via resonant tunneling between the Fe ions and one of its RG nearest neighbors. As a consequence of this process, excited Fe^{n+} states will be formed, which may have a lifetime much longer than the nuclear lifetime τ_γ. The isomer shift of such metastable states can *not* be taken as isomer-shift calibration points as long as DFS calculations for $\rho(0)$ of such excited states are not available. Nevertheless, using only electronic ground-state configurations [$Fe(3d^6 4s^2)$, $Fe^{+}(3d^6 4s)$] and the weakly excited $(Fe^{+})^*(3d^7)$ state in Ar together with DFS calculations available for these Fe configurations, we get a new $\Delta\langle r^2\rangle$ value for ^{57}Fe which is in rather good agreement with that obtained from lifetime measurements of the ^{52}Fe EC decay.

---

*Permanent address: Institut für Experimentalphysik IV, Ruhr-Universität, D-4630 Bochum, West Germany.

†Permanent address: Soreq Nuclear Research Centre, Yavne, Israel.

[1]For a review on this subject, see, H. Coufal, E. Lüscher, and H. Micklitz, in *Rare Gas Solids,* Vol. 103 of *Springer Tracts in Modern Physics,* edited by G. Höhler (Springer, Berlin, 1984), p. 1–57.

[2]H. Micklitz and P. H. Barrett, Phys. Rev. Lett. **24**, 1547 (1972).

[3]M. Van Rossum, J. Odeurs, H. Pattyn, J. De Troyer, E. Verbiest, R. Coussement, and S. Bukshpan, Phys. Lett. 75A, 241 (1980).

[4]The ^{57}Co(Ar) spectrum at 4.2 K published together with all the spectra of ^{57}Co in Ne, N_2, and CH_4 in a preliminary paper (M. Van der heyden, M. Pasternak, and G. Langouche, Proceedings of the International Conference on the Applications of the Mössbauer Effect, Leuven, 1985 [Hyperfine Interact. **29**, 1315 (1986)]) showed a strong ME resonance line around zero velocity. These experiments had been performed in a high-vacuum liquid-helium cryostat ($p \approx 10^{-4}$ Pa without liquid He in the cryostat). Since it is known from earlier experiments (see Ref. 3) that residual gas impurities (probably O_2) can cause an impurity line around zero velocity we were suspicious about the reliance of these preliminary spectra and have repeated the experiments in UHV ($p \approx 10^{-6}$ Pa without liquid He in the cryostat). Under these conditions the zero-velocity line appeared no more in any of these spectra. From this we came to the conclusion that the spectra shown in our preliminary paper are not correct.

[5]H. Micklitz and F. J. Litterst, Phys. Rev. Lett. **33**, 480 (1974).

[6]P. A. Montano, P. H. Barrett, H. Micklitz, A. F. Freeman, and F. V. Mallow, Phys. Rev. B **17**, 6 (1978).

[7]H. Micklitz, M. Van der heyden, and G. Langouche, Europhys. Lett. (to be published).

[8]T. K. McNab, H. Micklitz, and P. H. Barrett, Phys. Rev. B **4**, 3787 (1971).

[9]H. Pollak, Phys. Status Solidi. **2**, 270 (1962).

[10]C. E. Moore, *Atomic Energy Levels II,* Natl. Bur. Stand. (U.S) Circ. No. 467 (U.S. GPO, Washington, D.C., 1952), Vol. II, p. 49.

[11]Actually, the rather broad $(^{57}Fe^{+})^*(3d^7)$ spectrum for Kr and Ar+10 at.% Xe does not allow to decide whether the observed line broadening is due to a magnetic or a quadrupolar hf interaction. In order to be consistent with the $(^{57}Fe^{+})^*(3d^7)$ spectrum in Ar at 17 K, which definitely did not show any quadrupolar broadening, we assume that the line broadening observed in Kr and Ar+(10 at.% Xe) also has a magnetic origin.

[12]C. K. Jen, V. A. Bowers, E. L. Cochran, and S. N. Foner, Phys. Rev. **126**, 1749 (1962).

[13]F. P. Goldsborough and T. R. Koehler, Phys. Rev. **133**, A135 (1964).

[14]L. B. Knight and W. Weltner, Jr., J. Chem. Phys. **55**, 5066 (1971).
[15]F. H. Ammeter and D. C. Schlosnagle, J. Chem. Phys. **59**, 4784 (1973).
[16]V. A. Apkarian (private communication).
[17]G. K. Wertheim and D. N. E. Buchanan, Phys. Rev. **161**, 478 (1967).
[18]G. K. Shenoy (unpublished).
[19]R. Reschke, A. Trautwein, and F. P. Desclaux, J. Phys. Chem. Solids **38**, 837 (1977).
[20]A. Meykens, R. Coussement, J. Ladrière, M. Cogneau, M. Bogé, P. Auric, R. Bouchez, A. Benabed and F. Godard, Phys. Rev. B **21**, 3816 (1980).